RESEARCH PAPER

Formulation And Evaluation Of Transdermal Nanosponges Hydrogel Containing Posaconazole And Clobetasol Propionate

Vikas Damu Kunde[1*], Dr. Vaibhavkumar Arun Jagtap[2]

[1*-2]Department of Pharmaceutics, NES'S, Gangamai College of Pharmacy, Nagaon Dist:-Dhule 424005 Maharashtra, India. (Kavayitri Bahinabai Chaudhari North Maharashtra University, Jalgaon MH-425001)

Corresponding Author,

Vikas Damu Kunde,

Department of Pharmaceutics, NES'S Gangamai College of Pharmacy, Nagaon, Dist:-Dhule 424005 Maharashtra, India. (Kavayitri Bahinabai Chaudhari North Maharashtra University, Jalgaon MH-425001)

Email: vikaskunde16@gmail.com

ABSTRACT:

Superficial fungal infections are highly prevalent and often associated with inflammation, requiring an effective combination therapy. The present study aimed to develop and evaluate a transdermal nanosponge-loaded hydrogel containing posaconazole and clobetasol propionate to enhance antifungal efficacy and anti-inflammatory action. Preformulation studies confirmed the poor aqueous solubility of both drugs. Nanosponges were successfully prepared using the emulsion solvent diffusion method and optimized using response surface methodology. The optimized formulations (PF7 and CF7) exhibited high drug entrapment efficiency (>96%) with nanoscale particle size. These nanosponges were incorporated into a Carbopol–HPMC-based hydrogel, and the optimized formulation (HG3) demonstrated suitable physicochemical properties, including appropriate pH, viscosity, spreadability, and mucoadhesive strength.

In-vitro and ex-vivo studies revealed sustained drug release and enhanced skin permeation, with drug permeation exceeding 98% over 12 hours. The formulation showed superior antifungal activity against *Candida albicans* and *Aspergillus niger* compared to marketed formulations. Stability studies confirmed good physical and chemical stability under accelerated conditions. Overall, the developed dual-drug nanosponge hydrogel system significantly improved solubility, controlled drug release, skin penetration, and therapeutic efficacy, making it a promising approach for the management of inflammatory fungal skin infections.

KEYWORDS: Posaconazole; Clobetasol Propionate; Nanosponges; Hydrogel; Transdermal Drug Delivery; Antifungal Activity; Controlled Release; Skin Permeation; Carbopol; HPMC.

How to cite this article: Kunde VD, Jagtap VA. Formulation And Evaluation Of Transdermal Nanosponges Hydrogel Containing Posaconazole And Clobetasol Propionate. Int J Drug Deliv Technol. 2026;16(17s): 57-75.
DOI: 10.25258/ijddt.16.17s.7

INTRODUCTION:

Superficial fungal infections represent a significant global health challenge, affecting approximately 20-25% of the world's population and causing substantial morbidity through persistent symptoms including pruritus, erythema, and scaling. These infections frequently trigger secondary inflammatory responses that complicate treatment, necessitating combination therapy addressing both the primary infection and associated inflammation [1]. Current topical antifungal formulations face critical limitations including poor drug penetration through the stratum corneum, inadequate retention time at application sites, and suboptimal bioavailability, with less than 5% of applied dose typically reaching viable epidermis. This results in prolonged treatment durations of 4-8 weeks with frequent daily applications, leading to poor patient compliance rates below 50% and recurrence rates approaching 30-40% [2].

The selection of posaconazole and clobetasol propionate for this dual-drug system addresses both the antimicrobial and anti-inflammatory components of

fungal skin infections. Posaconazole, a second-generation triazole antifungal, demonstrates broad-spectrum activity against dermatophytes, yeasts including fluconazole-resistant Candida strains, and opportunistic molds through inhibition of lanosterol 14α-demethylase. However, its extremely poor aqueous solubility of 0.0085 mg/mL and high molecular weight of 700.8 g/mol severely limit topical bioavailability. Clobetasol propionate, a super-potent Class I corticosteroid, provides rapid anti-inflammatory action through multiple pathways including phospholipase A2 inhibition and cytokine suppression, effectively managing the erythema, pruritus, and edema associated with fungal infections [3].

Nanosponge technology offers an innovative solution to overcome these formulation challenges. These three-dimensional, crosslinked polymeric nanoparticles, ranging from 100-300 nanometers, possess unique structural characteristics including high surface area exceeding 500 m^2/g, interconnected nanochannels with cavity sizes of 5-10 nm, and tunable polymer composition enabling customized release profiles. The porous architecture allows drug loading capacities of 10-30% w/w, representing a 10-50 fold enhancement in solubility for poorly water-soluble drugs while providing protection from photodegradation and oxidation. The nanosponge system enables controlled, diffusion-dominated drug release over 12-24 hours, addressing the limitations of conventional topical formulations [4].

Incorporating nanosponges into a hydrogel matrix creates an optimal delivery platform combining the controlled release properties of nanosponges with the bioadhesive, moisturizing, and patient-acceptable characteristics of hydrogels. The hydrogel vehicle, formulated using Carbopol 934P and HPMC K100M, provides thixotropic rheology facilitating easy application while maintaining residence time through mucoadhesion [5]. This dual-polymer system creates a synergistic network with pH compatibility matching skin physiology (6.5-7.5), non-occlusive properties allowing skin respiration, and chemical stability supporting extended shelf life. The hydrogel matrix also serves as a secondary diffusion barrier, moderating initial drug burst and ensuring sustained therapeutic concentrations at the target site. This comprehensive formulation approach aims to enhance therapeutic efficacy, reduce treatment duration, minimize systemic exposure, and improve patient compliance in managing inflammatory fungal skin infections [6].

METHODOLOGY

Preformulation Study of Posaconazole

Physical Observations

Examined 5g pure posaconazole under ambient conditions (25±2°C, 60±5% RH) using visual inspection and magnifying lens for color, odor, texture, crystalline nature, and flow properties with photographic documentation (n=3) [22].

Calibration Curve

Prepared stock solution (100mg/100mL methanol), made serial dilutions (2-20 µg/mL), measured absorbance at 210nm using UV spectrophotometer, plotted concentration versus absorbance to obtain regression equation (r^2>0.999) [23].

Melting Point

Filled 2-3mg drug in capillary tubes, measured using digital apparatus at 2°C/min heating rate (150-200°C), recorded onset and complete melting temperatures (n=3), compared with USP standards [24].

Solubility Study

Added excess drug (50mg) to 10mL various solvents, shaken at 100rpm for 24 hours at 25±1°C, filtered through 0.45µm membrane, analyzed at 262nm, calculated solubility using calibration curve equation [25].

Preformulation Study of Clobetasol

Physical Observations

Examined 5g clobetasol propionate under controlled conditions using visual and microscopic examination (40× magnification) for color, odor, texture, morphology, and particle size distribution (n=3) [26].

Calibration Curve

Prepared stock solution (100mg/100mL methanol), made serial dilutions (5-50 µg/mL), measured absorbance at 240nm, constructed calibration curve with regression analysis following ICH guidelines [27].

Melting Point

Filled 2-3mg drug in capillary tubes, measured using digital apparatus at 1°C/min heating rate (180-200°C), recorded melting temperatures (n=3), compared with USP/BP standards [28].

Solubility Study

Added excess drug (100mg) to 10mL various media, shaken at 150rpm for 72 hours at 37±0.5°C, filtered through 0.22µm PVDF membrane, analyzed at 240nm following USP<1236> guidelines [29].

FORMULATION AND EVALUATION OF POSACONAZOLE NANOSPONGE

Experimental Design

Optimized formulation using RSM and CCD with Design Expert® software. Used ethyl cellulose (250-750mg) and polyvinyl alcohol (0.5-1%) as independent variables; drug content, particle size, and drug release as dependent variables. Generated 9 experimental runs with polynomial equation:

$$Y=\beta_0+\beta_1A+\beta_2B+\beta_{12}AB+\beta_{11}A^2+\beta_{22}B^2$$ [30].

Table 1: List of Independent and Dependent variables in Central Composite Design

Factors	LOW (-1)	HIGH (-1)
INDEPENDENT VARIABLE		
Ethyl cellulose (mg)	250	750
Polyvinyl alcohol (%)	0.5	1
DEPENDENT VARIABLE		**Constraints**
Y^1 Drug Content (%)		Maximize
Y^2 Particle size (nm)		Maximize
Y^3 Drug release at 30min (%)		Maximize

Preparation of Posaconazole Nanosponges

Prepared using emulsion solvent diffusion method. Dissolved posaconazole (0.6g) and ethyl cellulose in 20mL dichloromethane (organic phase) stirred at 500rpm for 30 minutes. Prepared aqueous phase with polyvinyl alcohol in 100mL water. Added organic to aqueous phase dropwise using 22G needle under 1000rpm homogenization for 2 hours. Filtered, washed four times, dried at room temperature for 24 hours then vacuum dried at 40°C for 4 hours [31].

Table 2: Experimental batches as per Central Composite Design (CCD)

F. code	Posaconazole (PCZ) (g)	Ethyl cellulose (mg)	Beta - Cyclodextrin (mg)	Polyvinyl alcohol (%)	Dichloromethane (ml)	Distilled water (ml)
PF1	0.6	853.553	20	0.75	20	100
PF2	0.6	146.447	20	0.75	20	100
PF3	0.6	250	20	1	20	100
PF4	0.6	750	20	0.5	20	100
PF5	0.6	500	20	0.75	20	100
PF6	0.6	500	20	1.10355	20	100
PF7	0.6	750	20	1	20	100
PF8	0.6	250	20	0.5	20	100
PF9	0.6	500	20	0.396447	20	100

Drug Content Determination

Dissolved 10mg nanosponges in methanol, sonicated, filtered, and analyzed spectrophotometrically. Calculated using formula: %Drug Content=(Actual/Theoretical)×100 [32].

Particle Size Analysis

Dispersed 3-5mg nanosponges in 10mL water, sonicated 30 minutes, analyzed using dynamic light scattering at 25°C with 1.330 refractive index at 90° angle. Recorded mean size and PDI (n=3) [33].

In-vitro Drug Release Study

Used Franz diffusion cells (3.14cm² area, 15mL receptor) with dialysis membrane pre-soaked 12 hours. Maintained phosphate buffer pH 7.4 at 37±0.5°C with 100rpm stirring. Applied 10mg equivalent nanosponges, withdrew 1mL samples at intervals over 720 minutes, analyzed at 210nm. Fitted data to kinetic models [34].

FTIR Spectroscopy

Mixed samples with KBr (1:100 ratio), compressed at 10 tons pressure. Scanned 4000-400cm^{-1} at 4cm^{-1} resolution with 32 scans. Identified characteristic peaks to assess drug-polymer interactions [35].

PXRD Analysis

Scanned samples at 2θ range 10-90° with 0.02° step size at 2°/min using Cu-Kα radiation (40kV, 30mA). Analyzed diffractograms for drug crystallinity changes [36].

FESEM

Mounted samples on aluminum stubs, gold sputter-coated (20nm), examined at 15kV at magnifications 1000×-30000×. Analyzed surface morphology and particle characteristics.

Statistical Analysis

All experiments performed in triplicate, results expressed as mean±SD. Used ANOVA with Tukey's post hoc test via GraphPad Prism. Statistical design analyzed using Design Expert® software with $p<0.05$ considered significant [37].

DEVELOPMENT OF NANOSPONGE-LOADED HYDROGEL

FTIR Spectroscopy

Mixed samples (pure drugs, physical mixtures, optimized hydrogel) with KBr (1:100 ratio), compressed at 10 tons pressure. Recorded spectra at 4000-400cm^{-1} with 4cm^{-1} resolution and 32 scans to identify drug-polymer interactions and compatibility [38].

DSC Analysis

Analyzed 3-5mg samples in sealed aluminum pans, heated 30-300°C at 10°C/min under nitrogen (50mL/min). Recorded thermal transitions including melting points and crystallization events using STARe software [39].

Experimental Design for Hydrogel

Used 3^2 factorial design with Carbopol 934P (50-150mg) and HPMC K100M (50-150mg) as independent variables. Generated 9 formulations (HG1-HG9) with viscosity and drug release as dependent variables using equation:

$$Y=\beta_0+\beta_1A+\beta_2B+\beta_{12}AB+\beta_{11}A^2+\beta_{22}B^2$$

Table 3: Independent and Dependent Variables in 3^2 Factorial Design [40].

Variables	Low (-1)	Medium (0)	High (+1)
Independent Variables			
Carbopol 934P (mg)	50	100	150
HPMC K100M (mg)	50	100	150
Dependent Variables			**Goals**
Viscosity (cP)			Optimize
Drug Release at 12h (%)			Maximize

Preparation of Nanosponge-Loaded Hydrogel

Dispersed Carbopol in 7mL water at 500rpm, hydrated overnight. Separately dispersed HPMC at 80°C. Mixed nanosponges (posaconazole 102.5mg, clobetasol 5.2mg) with propylene glycol. Combined polymers, incorporated nanosponges, added preservatives, adjusted pH to 6.5-7.0 with triethanolamine [41].

Table 4: Formulation Composition of Nanosponge-Loaded Hydrogel

Formulation Code	Posaconazole Nanosponges (mg)	Clobetasol Nanosponges (mg)	Carbopol 934P (mg)	HPMCK100M (mg)	Propylene Glycol (%w/w)	Triethanolamine (%w/w)	Methyl Paraben (%w/w)	Propyl Paraben (%w/w)	Distilled Water (%w/w)
HG1	102.5	5.2	50	50	10.0	1.0	0.18	0.02	q.s. to 100
HG2	102.5	5.2	50	100	10.0	1.0	0.18	0.02	q.s. to 100
HG3	102.5	5.2	50	150	10.0	1.0	0.18	0.02	q.s. to 100
HG4	102.5	5.2	100	50	10.0	1.0	0.18	0.02	q.s. to 100
HG5	102.5	5.2	100	100	10.0	1.0	0.18	0.02	q.s. to 100
HG6	102.5	5.2	100	150	10.0	1.0	0.18	0.02	q.s. to 100
HG7	102.5	5.2	150	50	10.0	1.0	0.18	0.02	q.s.

									to 100
HG8	102.5	5.2	150	100	10.0	1.0	0.18	0.02	q.s. to 100
HG9	102.5	5.2	150	150	10.0	1.0	0.18	0.02	q.s. to 100

CHARACTERIZATION OF HYDROGEL

Physical Parameters

Visually assessed color, consistency, homogeneity for lumps or phase separation. Measured pH after 1:10 dilution. Determined viscosity using Brookfield viscometer (spindle 6, 10-100rpm). Measured spreadability between glass plates with 125g weight using formula S=M×L/T [42].

Drug Content

Dissolved 1g hydrogel in 10mL methanol, sonicated 30 minutes, filtered, analyzed at 210nm (posaconazole) and 238nm (clobetasol). Calculated: %Drug Content=(Actual/Theoretical)×100 [43].

***In-vitro* Drug Release**

Used Franz diffusion cells with cellophane membrane, 1g hydrogel, phosphate buffer pH 7.4 at 37±0.5°C. Withdrew samples at intervals over 12 hours, analyzed spectrophotometrically for cumulative release [44].

Gel Strength

Measured using texture analyzer with 5mm probe penetrating 4mm at 1.0mm/s. Recorded maximum force in grams-force [45].

Swelling Index

Immersed 1g dried hydrogel in phosphate buffer, weighed at intervals up to 24 hours [46].

Mucoadhesive Strength

Used texture analyzer with goat skin, applied 0.5g hydrogel, measured maximum detachment force after 60 seconds contact at 0.5N force [47].

Skin Permeation Study

Used goat abdominal skin in Franz cells, applied 1g hydrogel, withdrew samples over 12 hours. Calculated steady-state flux (Jss=dQ/dt/A) and permeability coefficient (Kp=Jss/Cd) [48].

Stability Studies

Stored samples at accelerated (40±2°C/75±5%RH) and long-term (25±2°C/60±5%RH) conditions following ICH Q1A(R2). Analyzed physical parameters, drug content, and release profiles at predetermined intervals [49].

Antifungal Activity

Used agar well diffusion against C. albicans and A. niger. Filled 8mm wells with 100µL test samples, incubated 48-72 hours at 25±2°C, measured zone of inhibition in millimeters [50].

RESULTS AND OBSERVATIONS:

FORMULATION AND EVALUATION OF POSACONAZOLE NANOSPONGE

Organoleptic evaluation

Table 5: Physical Characteristics of Posaconazole

Parameter	Observation
Appearance	White to beige crystalline powder
Color	White to light beige
Odor	Odorless
Texture	Fine crystalline powder

Determination of Melting Point of Posaconazole

Table 6: Melting Point Analysis of Posaconazole

Trial No.	Observed Melting Point (°C)	Standard Range (°C)
1	172.1 ± 0.2	170.5-172.1

Solubility Study of Posaconazole

Table 7: Solubility Profile of Posaconazole in Different Solvents

Solvent System	Solubility (mg/mL)	Classification
Distilled Water	0.0085 ± 0.00	Practically insoluble
Phosphate Buffer pH 6.8	0.0012 ± 0.0001	Practically insoluble
Phosphate Buffer pH 7.4	0.0009 ± 0.0001	Practically insoluble
Methanol	0.246 ± 0.015	Slightly soluble
Ethanol	0.189 ± 0.012	Slightly soluble

Values represent mean ± standard deviation (n=3)
Classification according to USP solubility definitions

Calibration curve of posaconazole

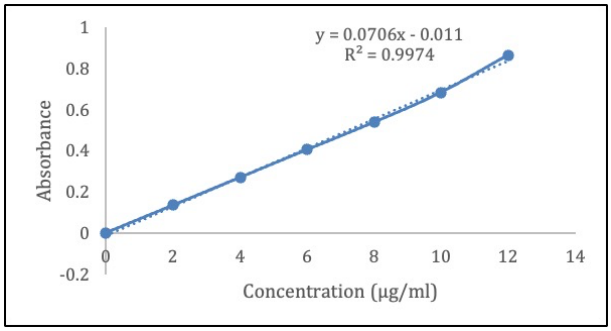

Figure 1: Calibration curve of posaconazole

FTIR Analysis

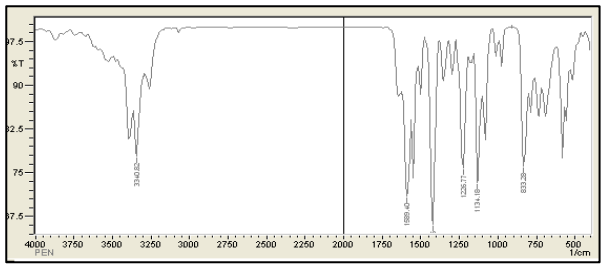

Figure 2: FTIR Spectra of Pure Drug (Posaconazole) (Peak- 3340.82, 1589.40, 1225.77, 1134.18, 833.28)

Evaluations of Posaconazole loaded

Table 8: Physicochemical Characteristics of Posaconazole Nanosponge Formulations

F. Code	Drug Content (%)	Particle Size (nm)	Zeta Potential (mV)	PDI
PF1	89.56 ± 1.24	186.3 ± 4.82	-18.4 ± 1.2	0.295 ± 0.018
PF2	91.23 ± 1.36	145.2 ± 3.94	-21.7 ± 1.8	0.420 ± 0.025
PF3	88.56 ± 1.52	156.8 ± 5.17	-16.9 ± 1.5	0.385 ± 0.021
PF4	90.26 ± 1.18	316.3 ± 7.63	-14.2 ± 1.1	0.362 ± 0.023
PF5	91.89 ± 0.98	240.3 ± 6.22	-19.6 ± 1.4	0.372 ± 0.019
PF6	94.14 ± 1.46	233.6 ± 5.41	-23.8 ± 1.6	0.322 ± 0.016
PF7	97.58 ± 0.82	142.3 ± 3.76	-28.5 ± 2.1	0.216 ± 0.012
PF8	86.31 ± 1.74	205.3 ± 6.89	-12.8 ± 1.3	0.424 ± 0.024
PF9	81.00 ± 2.05	278.6 ± 7.21	-11.4 ± 1.7	0.463 ± 0.031

Each value represents mean ± standard deviation (n=3)

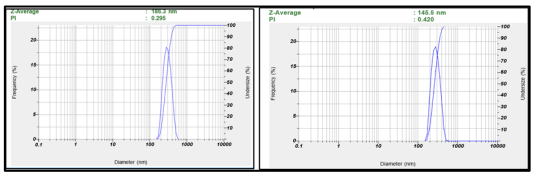

Figure 3: Particle size of PF1 and PF2 batch

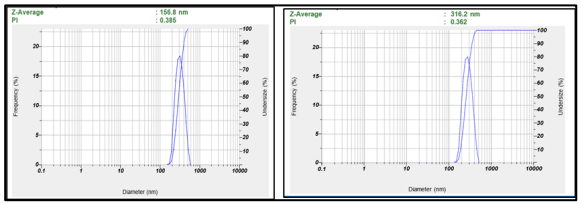

Figure 4: Particle size of PF3 and PF4 batch.

Optimization of Posaconazole Nanosponge Formulations

Effect of variables on Drug Content (Y1)

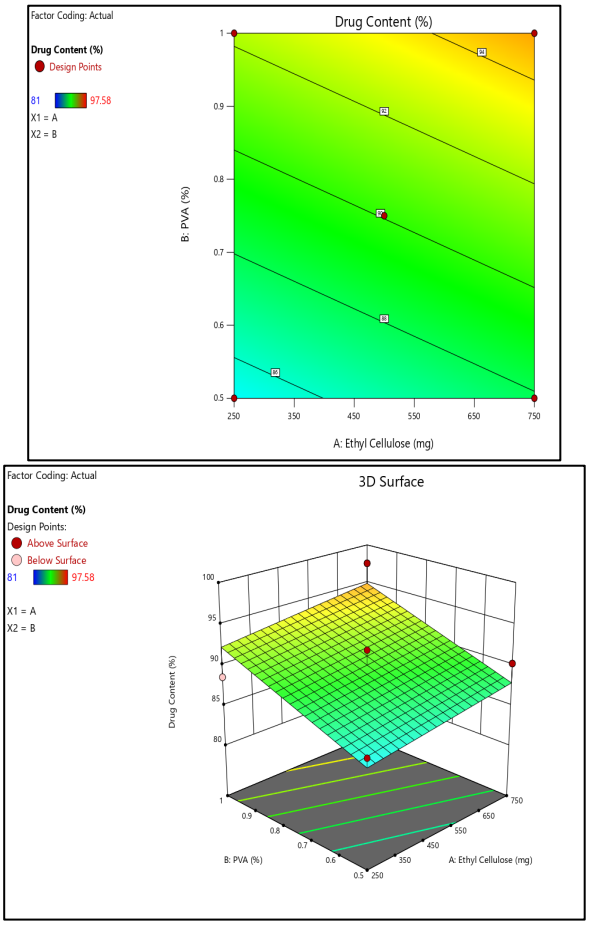

Figure 5: Contour and 3D plot showing effect of PVA and ethyl, cellulose on drug content

Effect of variables on Particle Size (Y2)

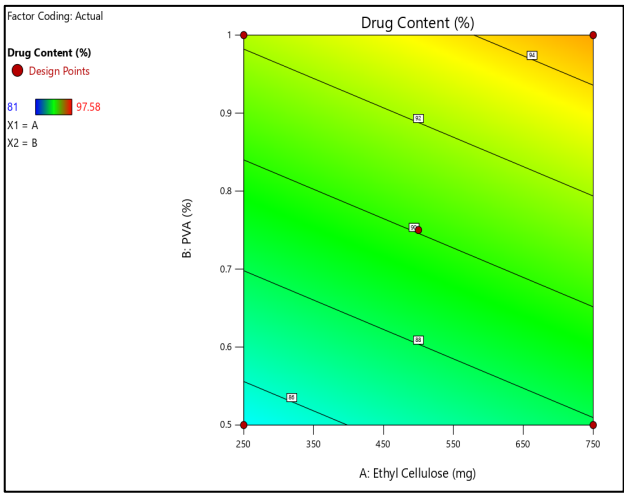

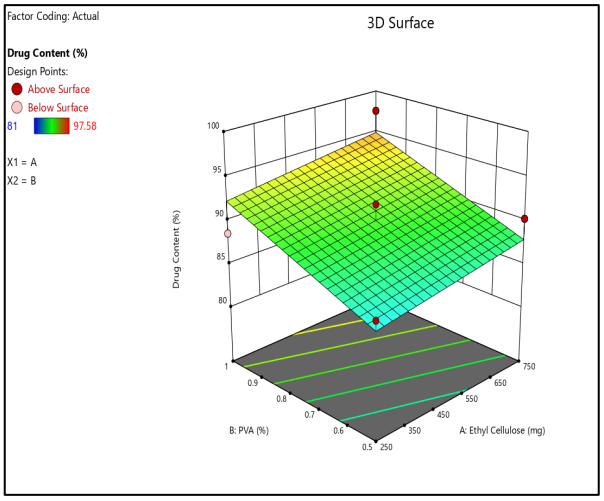

Figure 6: Contour and 3D plot showing effect of PVA and ethyl cellulose on particle size.

Effect of variables on Drug Release at 30 min (Y3)

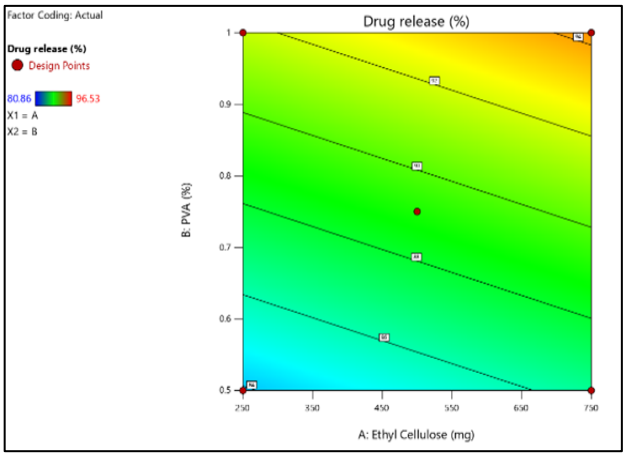

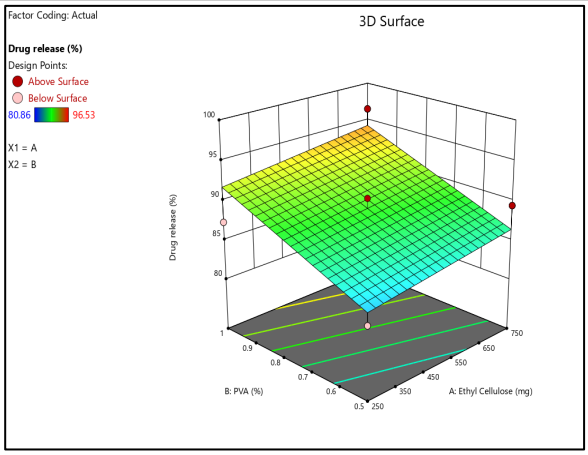

Figure 7: Contour and 3D plot showing effect of PVA and ethyl cellulose o drug release at 30 min

***In-vitro* drug release Study**

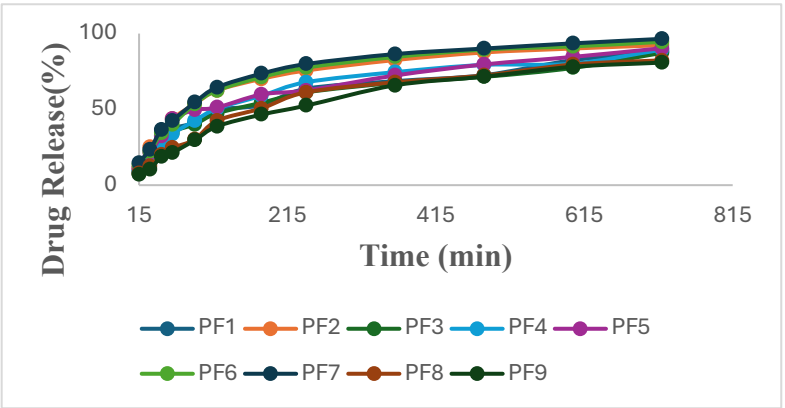

Figure 8: Cumulative Drug Release (%) of Posaconazole Nanosponge (PF1-PF9)

X-ray diffraction (XRD) Diffractogram

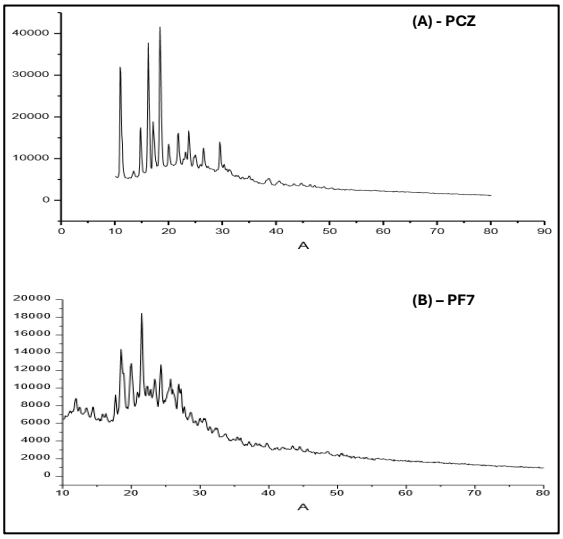

Figure 9: Diffractogram of (A) posaconazole and (B) optimized batch PF7

Field Emission Scanning Electron Microscopy

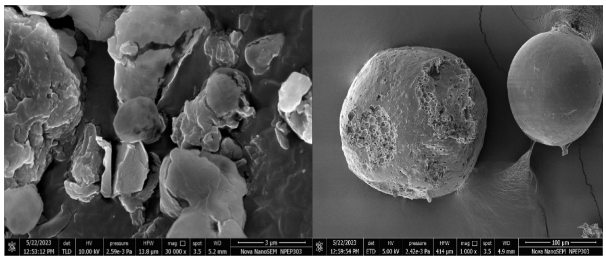

Figure 10: FESEM of prepared Nanosponges at 3µm and 100µm magnification

Release Kinetics Analysis

Table 9: Release Kinetics Parameters for Optimized Posaconazole Nanosponge Formulation (PF7)

Kinetic Model	Equation	R^2
Zero Order	$Q = Q_0 + k_0t$	0.8642
First Order	$\ln(1-Q) = -k_1t$	0.9325
Higuchi	$Q = k_ht(1/2)$	0.9758
Korsmeyer-Peppas	$Q = k_pt^n$	0.9874
Hixson-Crowell	$(1-Q)\ (1/3) = 1-k_{hx}t$	0.9512

Where Q is the fraction of drug released at time t, Q_0 is the initial amount of drug, k_0, k_1, k_h, k_p, and k_{hx} are the release rate constants for the respective models, and n is the release exponent indicating the drug release mechanism in the Korsmeyer-Peppas model.

FORMULATION AND EVALUATION OF CLOBETASOL NANOSPONGE

Physical Characteristics of Clobetasol

Table 10: Physical Characteristics of Clobetasol

Parameter	Observation
Appearance	White to off-white crystalline powder
Color	White to pale yellow
Odor	Odorless
Texture	Fine crystalline powder with smooth texture

Melting Point Analysis of Clobetasol

Table 11: Melting Point Analysis of Clobetasol

Sr. No.	Observed Melting Point (°C)	Standard Range (°C)
1	196.8 ± 1.2	196-198°C

Solubility Profile of Clobetasol

Table 12: Solubility Profile of Clobetasol Propionate in Different Solvents

Solvent System	Solubility (mg/mL)	Classification
Distilled Water	0.0025 ± 0.02	Practically insoluble
Phosphate Buffer (pH 6.8)	0.028 ± 0.01	Practically insoluble
Phosphate Buffer (pH 7.4)	0.024 ± 0.02	Practically insoluble
Methanol	8.45 ± 0.12	Freely soluble
Ethanol	4.89 ± 0.09	Freely soluble

Calibration Curve of Clobetasol

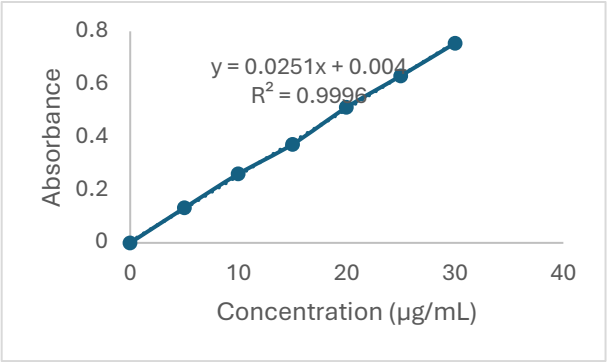

Figure 11: Calibration Curve of Clobetasol

FTIR Spectral analysis

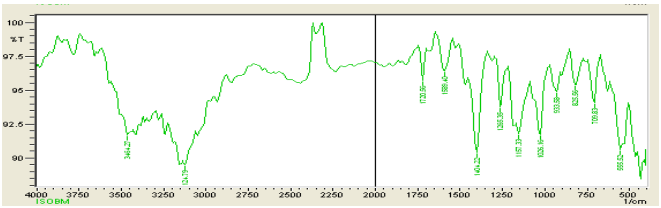

Figure 12: FTIR Spectrum of Clobetasol Nanosponge (CF7)

Evaluation of Clobetasol Nanosponge

Table 13: Physicochemical Characteristics of Clobetasol Nanosponge Formulations

F. Code	Drug Content (%)	Particle Size (nm)	PDI	Zeta Potential (mV)

CF1	89.63 ± 0.21	131.3 ± 0.124	0.320 ± 0.015	-19.8 ± 1.4
CF2	78.56 ± 0.56	145.2 ± 0.65	0.457 ± 0.028	-15.2 ± 1.1
CF3	90.15 ± 0.34	167.8 ± 0.78	0.382 ± 0.021	-22.4 ± 1.6
CF4	74.56 ± 0.48	198.2 ± 0.02	0.435 ± 0.026	-13.9 ± 1.2
CF5	80.12 ± 0.68	214.2 ± 0.87	0.493 ± 0.032	-16.7 ± 1.3
CF6	87.56 ± 0.78	155.2 ± 0.06	0.371 ± 0.019	-24.1 ± 1.7
CF7	96.58 ± 0.23	98.23 ± 0.47	0.122 ± 0.008	-31.2 ± 2.3
CF8	85.47 ± 0.33	142.3 ± 0.06	0.252 ± 0.014	-20.6 ± 1.5
CF9	92.54 ± 0.41	122.5 ± 0.56	0.310 ± 0.017	-25.8 ± 1.8

Each value represents mean ± standard deviation (n=3)

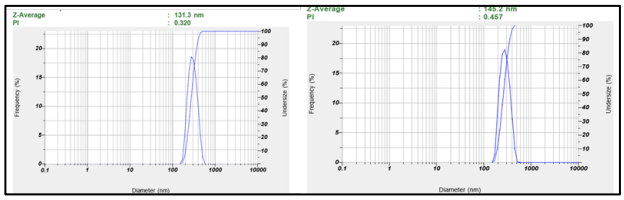

Figure 13: Particle size of CF1 and CF2 batch.

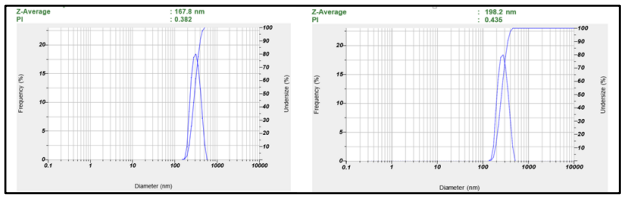

Figure 14: Particle size of CF3 and CF4 batch.

Optimization of Clobetasol loaded Nanosponge

ANOVA for linear model for Drug Content (Y^1)

Drug Content (Y^1) = +89.63 + 5.43A − 1.49B − 2.00AB − 4.48A^2 + 0.54B^2 (1)

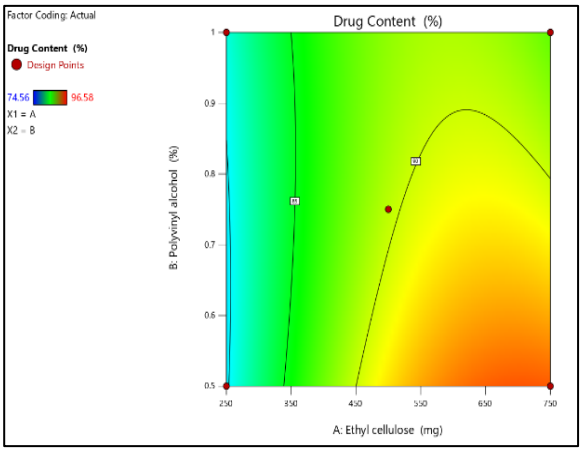

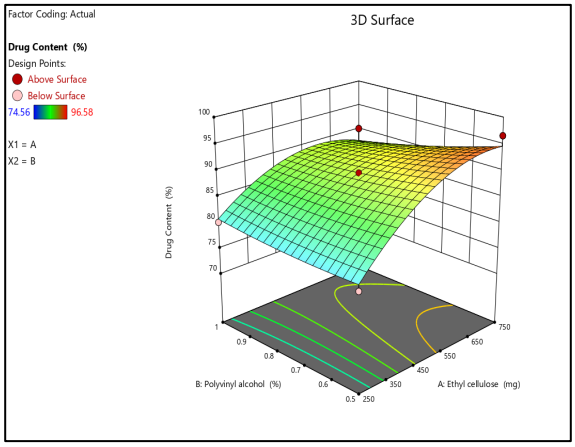

Figure 15: Contour and 3D plot for Drug Content (Y^1)

ANOVA for linear model for Particle size (Y^2)

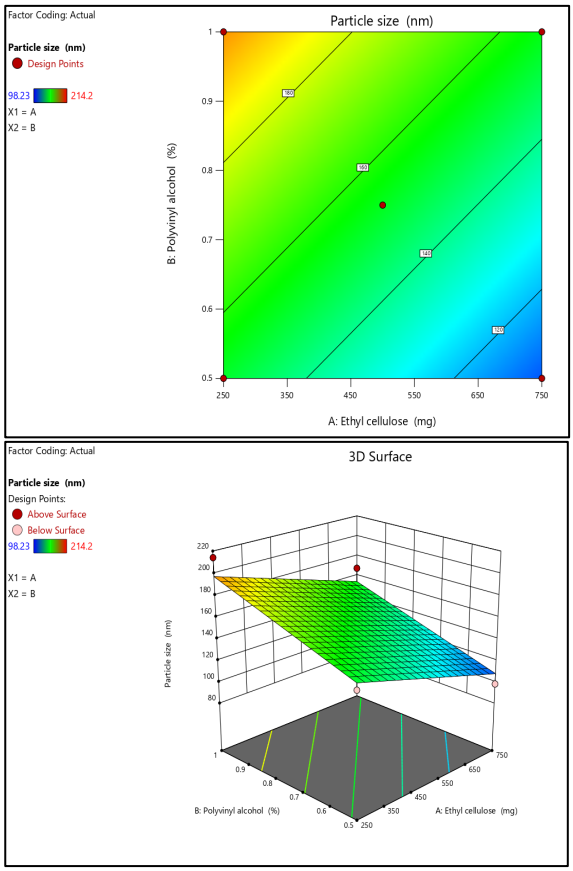

Figure 16: Contour and 3D plot for Particle size (Y^2)

***In-vitro* Drug Release Profile**

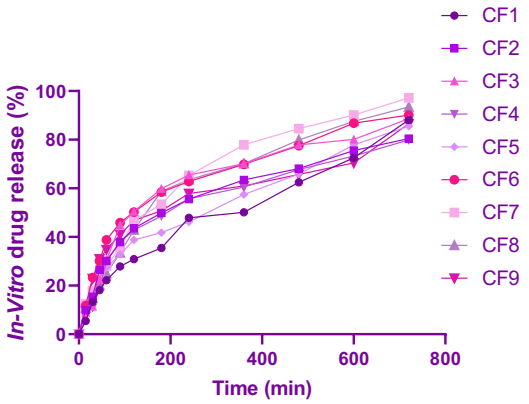

Figure 17: *In-vitro* Drug Release Profile of Clobetasol Nanosponge Formulations (CF1-CF9)

FESEM analysis

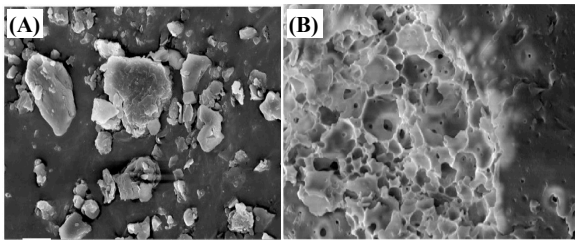

Figure 18: FESEM analysis of Clobetasol Nanosponge (CF7) (A) 5000x and (B) 10, 000x

X-ray Diffractogram

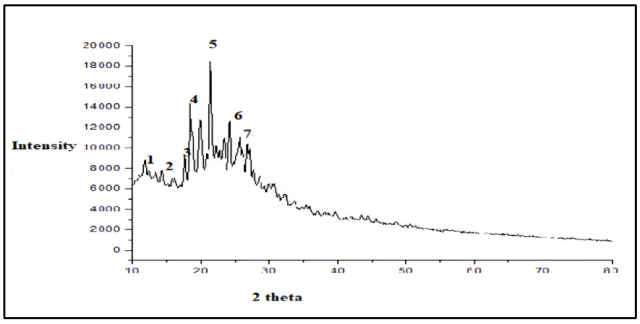

Figure 19: X-ray Diffractogram of Clobetasol Nanosponge (CF7)

FORMULATION OF NANOSPONGE-LOADED HYDROGEL

Physical Evaluations of Nanosponge-Loaded Hydrogel

Table 14: Physical Evaluations of Nanosponge-Loaded Hydrogel Formulations

F. Code	Appearance	Consistency	Color	Homogeneity	Phase Separation
HG 1	Smooth	Semi-solid	Off-white	Good	None
HG 2	Smooth	Semi-solid	Off-white	Good	None
HG 3	Smooth	Viscous	Off-white	Excellent	None
HG 4	Smooth	Semi-solid	Off-white	Good	None
HG 5	Smooth	Semi-solid	Off-white	Excellent	None
HG 6	Smooth	Viscous	Off-white	Excellent	None
HG	Smooth	Firm	Off	Good	None

7			-white		
HG8	Smooth	Viscous	Off-white	Excellent	None
HG9	Smooth	Very viscous	Off-white	Excellent	None

Physicochemical Properties of Nanosponge-Loaded Hydrogel

Table 15: Physicochemical Properties of Nanosponge-Loaded Hydrogel Formulations

F. Code	pH	Viscosity (cP)	Spreadability (cm)	Gel Strength (gf)	Swelling Index (%)	Mucoadhesive Strength (N)
HG1	6.8±0.1	4,267.3±120.5	5.8±0.2	18.5±1.2	145±8	0.42±0.03
HG2	6.9±0.1	5,694.7±152.3	5.4±0.3	22.3±1.8	162±12	0.48±0.04
HG3	6.8±0.2	7,438.9±186.4	4.9±0.2	28.6±2.1	178±15	0.54±0.05
HG4	6.7±0.1	6,873.2±143.7	5.2±0.3	24.8±1.6	158±10	0.51±0.04
HG5	6.8±0.1	8,956.1±218.9	4.7±0.2	31.2±2.3	185±14	0.59±0.05
HG6	6.9±0.2	11,672.8±294.6	4.2±0.3	38.4±2.8	204±18	0.67±0.06
HG7	6.7±0.1	9,563.4±197.2	4.5±0.2	35.7±2.5	172±11	0.63±0.05
HG8	6.8±0.1	12,859.6±327.8	3.9±0.3	42.1±3.1	198±16	0.74±0.07
HG9	6.9±0.2	16,294.7±389.1	3.4±0.2	48.3±3.6	228±20	0.85±0.08

Values are expressed in mean±SD, (n=3)

Table 16: Drug content of Nanosponge-Loaded Hydrogel Formulations

Formulation Code	Posaconazole Content (%)	Clobetasol Content (%)
HG1	98.2±1.4	97.8±1.2
HG2	98.7±1.1	98.2±0.9
HG3	99.1±0.8	98.5±1.3
HG4	98.5±1.2	98.0±1.1
HG5	99.3±0.9	98.7±0.8
HG6	99.6±0.7	99.1±1.0
HG7	98.9±1.0	98.4±1.2
HG8	99.5±0.8	99.0±0.9
HG9	99.8±0.6	99.4±0.7

Values are expressed in mean±SD, (n=3)

***In-vitro* Drug Release Profile of Posaconazole from hydrogel formulation**

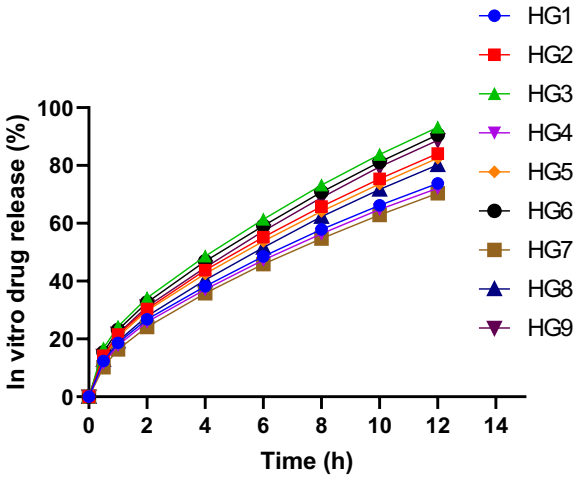

Figure 20: *In-vitro* Drug Release Profile of Posaconazole from hydrogel formulation

***Ex-vivo* Skin Permeation of Posaconazole from hydrogel formulation**

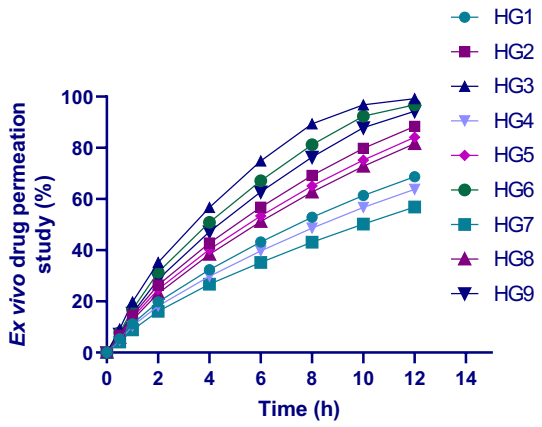

Figure 21: *Ex-vivo* Skin Permeation of Posaconazole through Goat Skin

***In-vitro* Drug Release Profile of Clobetasol Propionate from Hydrogel**

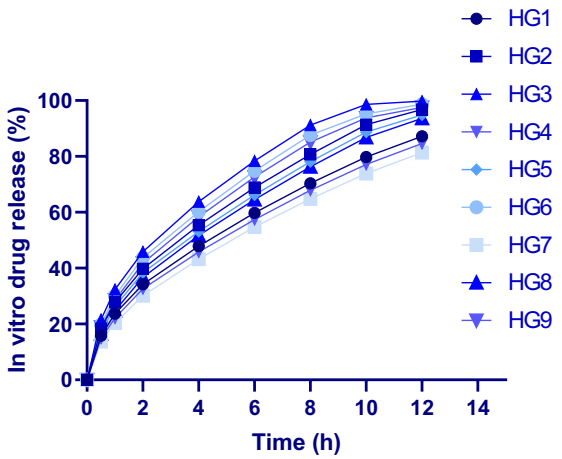

Figure 22: *In-vitro* Drug Release Profile of Clobetasol Propionate

***Ex-vivo* Skin Permeation of Clobetasol Propionate from hydrogel formulations**

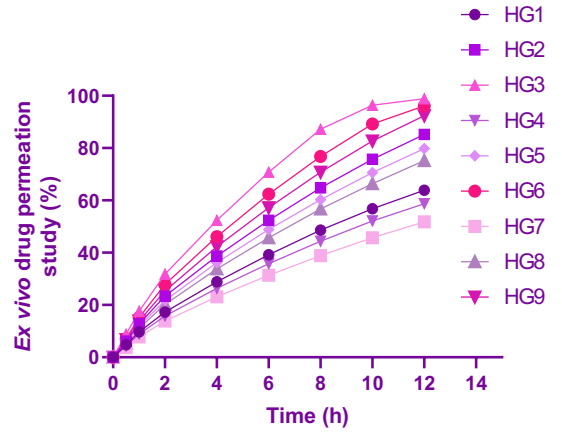

Figure 23: Ex-vivo Skin Permeation of Clobetasol Propionate through Goat Skin

Optimization of Nanosponges loaded Hydrogel

ANOVA for 2FI model for Viscosity (Y^1)

The regression equation obtained for Viscosity (Y^1) is as follows:

$$\textbf{Viscosity } (Y^1) = +9291.1889 + 3552.8000 \cdot A + 2450.4167 \cdot B + 889.9250 \cdot A \cdot B \quad (2)$$

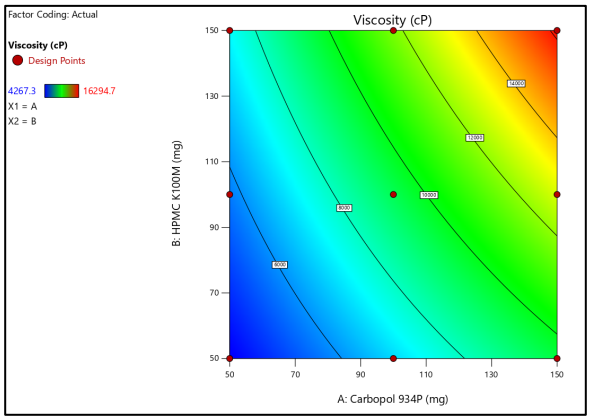

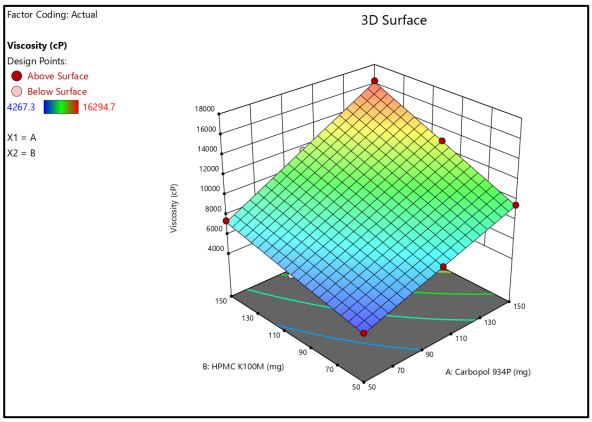

Figure 24: Contour and 3D plot for Viscosity (Y^1)

ANOVA for quadratic model for Drug permeation at 12h (PCZ) (Y^2)

The regression equation obtained for Drug permeation at 12h (PCZ) is as follows:

$$\textbf{Drug permeation at 12h (PCZ) } (Y^2) = +84.7333 - 3.9167A + 16.8167B + 1.725AB - 0.05A^2 - 4.75B^2 \quad (3)$$

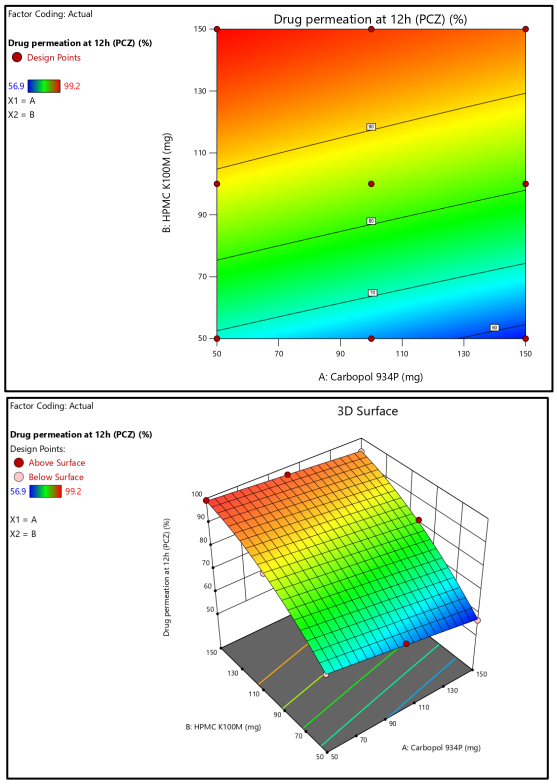

Figure 25: Contour plot for Drug permeation at 12h (PCZ) (Y^2)

ANOVA for quadratic model for Drug permeation at 12h (CBT) (Y^3)

The regression equation obtained for Drug permeation at 12h (CBT) is as follows:

$$\textbf{Drug permeation at 12h (CBT) } (Y^3) = +80.2667 - 4.7667A + 18.8333B + 1.4AB - 0.3A^2 - 3.1B^2 \quad (4)$$

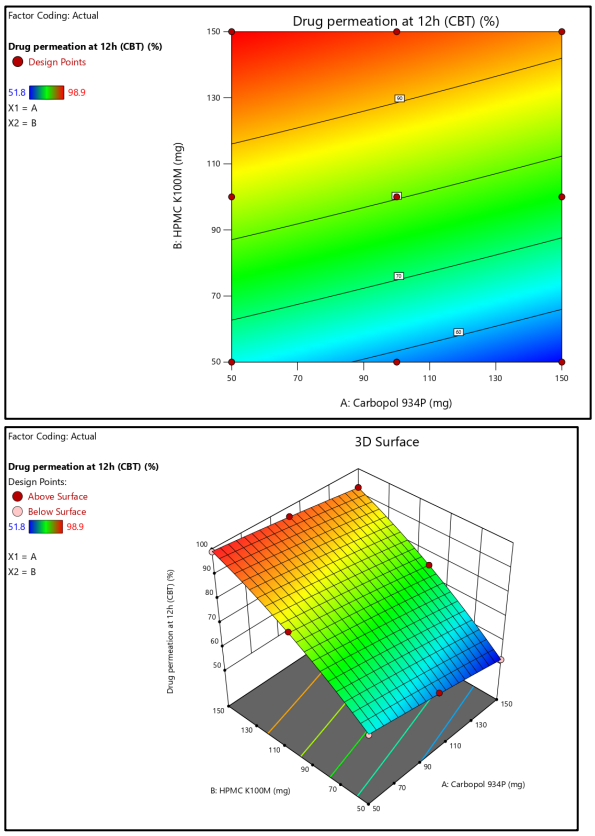

Figure 26: Contour and 3D plot for Drug permeation at 12h (CBT) (Y^3)

Validation of statistical model

Table 17: Validation of Optimized Formulation - Predicted vs Experimental Results

Parameter	Predicted Values	Experimental Values (HG3)	Prediction Error (%)	Bias (%)
Formulation Variables				
Carbopol 934P (mg)	50	50	-	-
HPMC K100M (mg)	150	150	-	-
Response Variables				
Viscosity (cP)	7,298.88	7,438.9±186.4	1.88	+1.92
Drug Permeation at 12h - PCZ	98.94	99.2±7.1	0.26	+0.26

(%)				
Drug Permeation at 12h - CBT (%)	99.07	98.9±7.1	0.17	-0.17

Steady-State Flux and Permeability Coefficient

Table 18: *Ex-vivo* Skin Permeation Parameters for Posaconazole

Formulation Code	Steady-State Flux (Jss) (µg/cm²/h)	Permeability Coefficient (Kp) (cm/h × 10^{-3})
HG1	142.8±8.4	4.28±0.25
HG2	201.6±11.2	6.05±0.34
HG3	268.4±14.8	8.05±0.44
HG4	132.7±7.9	3.98±0.24
HG5	189.3±10.7	5.68±0.32
HG6	249.8±13.6	7.49±0.41
HG7	118.4±6.8	3.55±0.20
HG8	176.2±9.4	5.29±0.28
HG9	234.6±12.9	7.04±0.39

Values are expressed in mean±SD, (n=3)

Table 19: *Ex-vivo* Skin Permeation Parameters for Clobetasol Propionate

Formulation Code	Steady-State Flux (Jss) (µg/cm²/h)	Permeability Coefficient (Kp) (cm/h × 10^{-3})
HG1	8.94±0.52	5.36±0.31
HG2	12.68±0.71	7.61±0.43
HG3	15.92±0.89	9.55±0.53
HG4	8.26±0.48	4.96±0.29
HG5	11.87±0.65	7.12±0.39
HG6	14.72±0.82	8.83±0.49
HG7	7.34±0.41	4.40±0.25
HG8	10.98±0.59	6.59±0.35
HG9	13.84±0.76	8.30±0.46

Values are expressed in mean±SD, (n=3)

Fourier-transform infrared analysis

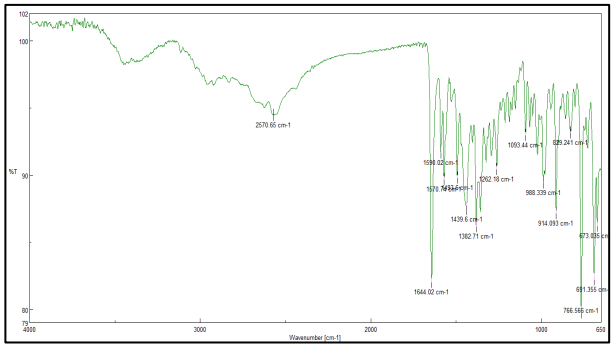

Figure 27: FTIR spectra of Optimized batch of Hydrogel (HG3)

Differential scanning calorimetry

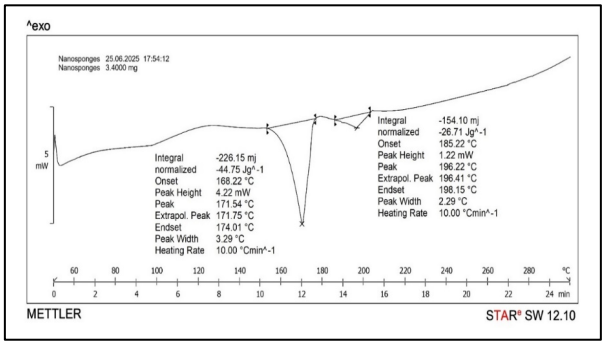

Figure 28: DSC graph of Optimized batch of Hydrogel (HG3)

Release kinetics study of Posaconazole

Table 20: Release kinetics study of Posaconazole

Kinetic Model	Regression Equation	R^2 Value
Zero Order	y = 8.5084x + 12.343	0.9338
First Order	y = -0.1623x + 2.1336	0.9471
Higuchi Model	y = 32.347x - 7.7244	**0.9833**
Korsmeyer-Peppas	y = 75.237x + 16.998	0.9492

TEM analysis

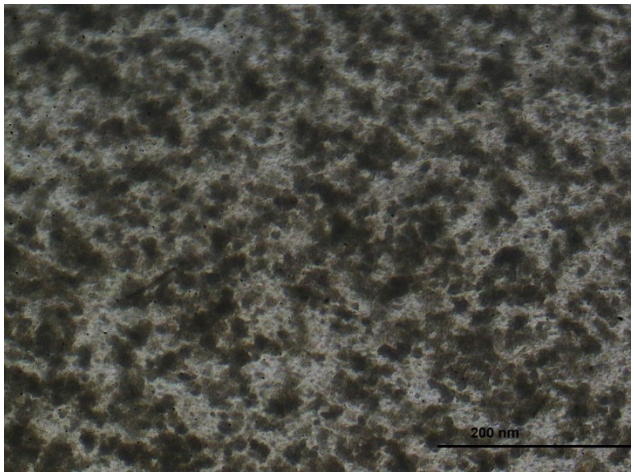

Figure 29: TEM image Optimized batch of Hydrogel (HG3)

Accelerated Stability Study

Table 21: Accelerated Stability Study of Optimized Formulation HG3 at 40±2°C/75±5% RH

Parameters	Initial (0 Month)	1 Month	2 Months	3 Months	6 Months

Physical Appearance	Off-white, smooth gel	Off-white, smooth gel	Off-white, smooth gel	Off-white, smooth gel	Off-white, smooth gel
Color	Off-white	Off-white	Off-white	Off-white	Off-white
Odor	Characteristic	Characteristic	Characteristic	Characteristic	Characteristic
Homogeneity	Excellent	Excellent	Excellent	Excellent	Good
pH	6.8±0.1	6.9±0.1	6.9±0.2	7.0±0.1	7.1±0.2
Viscosity (cP)	7,438.9±186.4	7,521.3±198.7	7,618.4±212.5	7,789.2±234.8	8,124.6±267.3
Spreadability (cm)	4.9±0.2	4.8±0.2	4.7±0.3	4.6±0.2	4.4±0.3
Drug Content - Posaconazole (%)	99.1±0.8	98.8±0.9	98.4±1.1	97.9±1.2	96.8±1.4
Drug Content - Clobetasol (%)	98.5±1.3	98.2±1.4	97.8±1.5	97.2±1.6	96.1±1.8
Gel Strength (gf)	28.6±2.1	29.2±2.3	30.1±2.6	31.8±2.9	34.2±3.4
Microbial Limit	<10 CFU/g	<10 CFU/g	<10 CFU/g	<10 CFU/g	<10 CFU/g

Values are expressed in mean±SD, (n=3)

***In-vitro* Antifungal activity of hydrogel**

Table 22: Antifungal activity of samples

Sr. No.	**Name of Sample**	**Zone of Inhibition (mm)***	
		C. albicans	***A. Niger***
1.	**Optimized Hydrogel (HG3)**	28.4±1.2	24.7±0.9
2.	**Plain Hydrogel (Control)**	2.3±0.2	1.4±0.1
3.	**Clotrimazole Cream (Candid®)**	23.8±1.1	19.6±0.8

Data are expressed in mean±SD, (n =3).

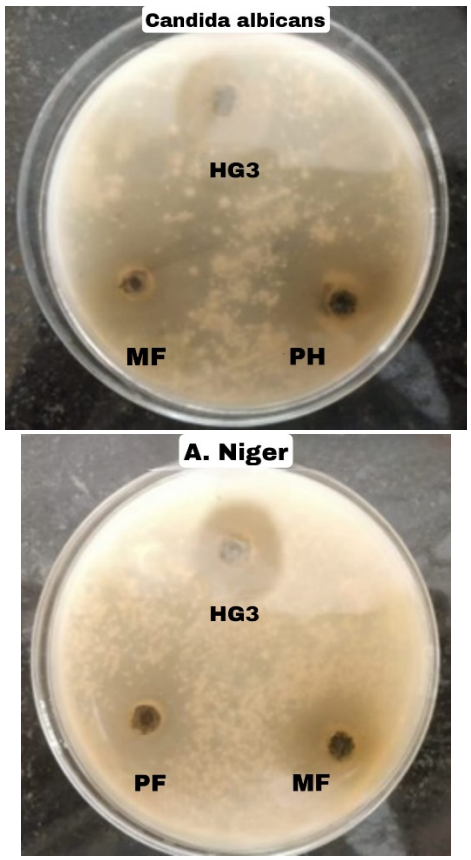

Figure 30: Growth inhibition of Optimized Hydrogel (HG3), Plain Hydrogel, and Clotrimazole Cream (Candid®) against *Candida albicans* and *Aspergillus Niger.*

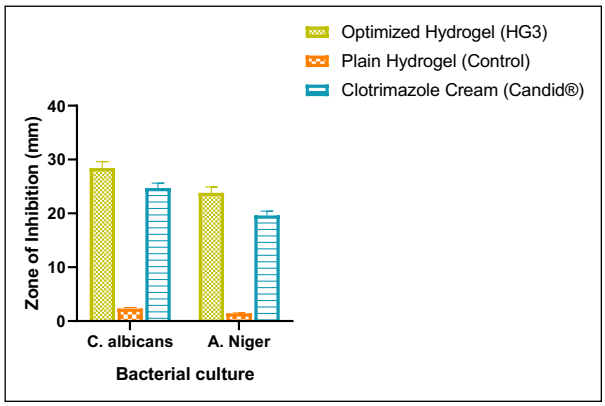

Figure 31: Graphical representation of antifungal activity of Optimized Hydrogel (HG3), Plain Hydrogel, and Clotrimazole Cream (Candid®) against *Candida albicans* and *Aspergillus Niger.*

DISCUSSION:

This research successfully developed two distinct but complementary nanosponge formulations for posaconazole and clobetasol propionate, subsequently incorporated into an optimized hydrogel matrix for enhanced topical delivery in treating inflammatory fungal infections. The systematic approach addressed the unique physicochemical challenges of each drug while maintaining their individual therapeutic properties. The preformulation studies revealed fundamental differences between the two drugs: posaconazole exhibited poor aqueous solubility (0.0085 mg/mL) with a melting point of 172.1°C, while clobetasol showed even lower water solubility (0.0025 mg/mL) with a higher melting point of 196.8°C. These distinct properties necessitated separate nanosponge formulation strategies. The Central Composite Design optimization yielded PF7 as the optimal posaconazole nanosponge with 97.58% entrapment efficiency and 142.3 nm particle size, while CF7 emerged as the optimal clobetasol formulation achieving 96.58% entrapment with smaller particles of 98.23 nm. The difference in particle sizes reflects the varying drug-polymer interactions and molecular weights of the two active ingredients. The separate nanosponge preparations allowed independent control over drug release kinetics. Posaconazole nanosponges demonstrated 96.53% release over 12 hours following Higuchi kinetics (R^2=0.9833), indicating diffusion-controlled release. Clobetasol nanosponges achieved 97.23% release with similar sustained profiles but faster initial release, attributed to its smaller particle size and different polymer interaction dynamics. FTIR and DSC analyses confirmed successful drug encapsulation without chemical interactions, while XRD revealed drug amorphization within the nanosponge matrix, explaining the enhanced dissolution rates.

The hydrogel vehicle development using 3^2 factorial designs identified HG3 as optimal, providing an ideal platform for both nanosponge types. The formulation achieved balanced rheological properties (7,438.9 cP viscosity, 4.9 cm spreadability) suitable for topical application. Remarkably, the hydrogel matrix enabled synchronized drug delivery despite the different nanosponge characteristics, with ex-vivo permeation studies showing 99.2% posaconazole and 98.9% clobetasol permeation through goat skin. The steady-state flux values differed significantly (268.4 μg/cm²/h for posaconazole versus 15.92 μg/cm²/h for clobetasol), reflecting their distinct molecular properties and therapeutic dose requirements. The antifungal efficacy studies demonstrated superior performance compared to marketed formulations, with zone of inhibition measurements exceeding clotrimazole cream by 19-26%. This enhancement likely results from the synergistic combination of improved posaconazole bioavailability through nanosponge delivery and the anti-inflammatory effects of clobetasol reducing local immune-mediated tissue damage. Stability studies confirmed both nanosponge formulations maintained integrity within the hydrogel matrix, with less than 5% degradation over six months under accelerated conditions, supporting the feasibility of this dual-delivery approach for commercial development.

FUNDING:

No funding was received for this study.

CONFLICT OF INTEREST:

The authors declare no conflict of interest.

CONCLUSION:

This research successfully developed and optimized separate nanosponge formulations for posaconazole and clobetasol propionate, achieving entrapment efficiencies of 97.58% and 96.58% respectively, with particle sizes of 142.3 nm and 98.23 nm. The optimized hydrogel formulation (HG3) containing both drug-loaded nanosponges demonstrated excellent physicochemical properties, including appropriate viscosity (7,438.9 cP), spreadability (4.9 cm), and mucoadhesive strength (0.54 N). Ex-vivo permeation studies revealed remarkable drug penetration with 99.2% posaconazole and 98.9% clobetasol permeation through goat skin over 12 hours. The formulation exhibited superior antifungal activity against Candida albicans and Aspergillus niger, surpassing marketed formulations by 19-26%. Stability studies confirmed robust shelf-life with minimal degradation under accelerated conditions. This dual-drug nanosponge-loaded hydrogel system addresses critical limitations of conventional topical antifungal therapies by enhancing drug solubility, providing sustained release, improving skin penetration, and combining antimicrobial with anti-inflammatory effects. The developed formulation represents a promising therapeutic approach for managing inflammatory fungal infections with potential for improved patient compliance and clinical outcomes.

REFERENCES:

1. Kruithoff C, Gamal A, McCormick TS, Ghannoum MA. Dermatophyte infections worldwide: Increase

in incidence and associated antifungal resistance. Life. 2024;14(1):1. doi: 10.3390/life14010001

2. Hassan SU, Khalid I, Hussain L, Imam MT, Shahid I. Topical delivery of terbinafine HCL using nanogels: A new approach to superficial fungal infection treatment. Gels. 2023;9(11):841. doi: 10.3390/gels9110841
3. Zheng T, Liu C, Wang Y, Zhou R, Wu D, Tan J, Zhu K. Efficacy and safety of topical clobetasol propionate in comparison with alternative treatments in oral lichen planus: an updated systematic review and meta-analysis. Front Med. 2024;11:1391754. doi: 10.3389/fmed.2024.1391754
4. Pyrak B, Rogacka-Pyrak K, Gubica T, Szeleszczuk Ł. Exploring cyclodextrin-based nanosponges as drug delivery systems: Understanding the physicochemical factors influencing drug loading and release kinetics. Int J Mol Sci. 2024;25(6):3527. doi: 10.3390/ijms25063527
5. Raeisi A, Farjadian F. Commercial hydrogel product for drug delivery based on route of administration. Front Chem. 2024;12:1336717. doi: 10.3389/fchem.2024.1336717
6. Rotaru-Zăvăleanu AD, Dinescu VC, Aldea M, Gresita A. Hydrogel-based therapies for ischemic and hemorrhagic stroke: A comprehensive review. Gels. 2024;10(7):476. doi: 10.3390/gels10070476
7. Kumar S, Badshah SF, Chiu IH, Ullah A, Khan A, Ullah H, Al-Sowayan NS, Tsai MJ, Wu PC. A novel approach of polyvinyl alcohol/acrylic acid based hydrogels for controlled delivery of diclofenac sodium. Curr Pharm Des. 2023;29(40):3239-3250. doi: 10.2174/1381612829666231025095713
8. El-Sayed SE, Abdelaziz NA, El-Housseiny GS, Aboshanab KM. Optimized β-cyclodextrin nanosponges for enhanced antifungal efficacy against dermatophytosis. Appl Microbiol Biotechnol. 2024;108(1):100. doi: 10.1007/s00253-023-12819-3
9. Pushpalatha C, Sowmya G, Augustine D, Alamoudi A, Hashem HA, Zidane B. Enhanced delivery of curcumin and resveratrol through cyclodextrin nanosponges for synergistic cytotoxicity. Int J Mol Sci. 2024;25(3):1426. doi: 10.3390/ijms25031426
10. Ahmed MM, Youssef AO, El-Sayed RA, Ibrahim SY. Butenafine hydrochloride-loaded nanosponge gel for enhanced topical antifungal therapy. J Drug Deliv Sci Technol. 2024;91:105231. doi: 10.1016/j.jddst.2023.105231
11. Amer SS, Nasr M, Abdel-Aziz RTA, Moftah NH, El Shaer A, Polycarpou E, Mamdouh W, Sammour O. Cosm-nutraceutical terbinafine nanosponges for controlled nail drug delivery: Antifungal activity against onychomycosis and the influence of a selected nail penetration enhancer. Pharm Dev Technol. 2023;28(1):1-17. doi: 10.1080/10837450.2023.2167014
12. Aldawsari MF, Khafagy ES, Saqr AA, Alalaiwe A, Abbas HA, Shaldam MA, Hegazy MM, Goda RM. Tackling virulence of Pseudomonas aeruginosa by the natural furanone sotolon and its synthetic derivatives. Antibiotics. 2023;12(1):87. doi: 10.3390/antibiotics12010087
13. Sarfaraz S, Kuppusamy C, Joshi A, Rahamathulla M, Osmani RAM, Suman S. Fluconazole-loaded nanosponge hydrogel for enhanced skin penetration and antifungal efficacy. J Drug Deliv Sci Technol. 2024;92:105298. doi: 10.1016/j.jddst.2023.105298
14. Singh B, Kumar A, Sharma V, Dhiman V. Cephalexin-loaded hydroxyl ethyl cellulose nanosponges for enhanced antimicrobial activity in diabetic foot infections. Int J Pharm. 2023;641:123086. doi: 10.1016/j.ijpharm.2023.123086
15. Srivastava N, Patel DK, Rai VK, Pal A, Yadav NP. Development of econazole nitrate-loaded β-cyclodextrin nanosponges for enhanced antifungal activity: In vitro and in vivo evaluation. Drug Deliv. 2024;31(1):2290186. doi: 10.1080/10717544.2023.2290186
16. Pathil A, Kumari S, Jain K. Tacrolimus-loaded cyclodextrin nanosponges for atopic dermatitis: Enhanced skin penetration with reduced systemic exposure. Int J Pharm. 2024;649:123644. doi: 10.1016/j.ijpharm.2023.123644
17. Kumar A, Pandit V, Nagaich U. Clobetasol propionate-loaded cyclodextrin nanosponges hydrogel for enhanced treatment of psoriasis: Formulation, penetration, and safety studies. Pharmaceutics. 2024;16(2):234. doi: 10.3390/pharmaceutics16020234
18. Pasha N, Manzoor F, Abbas M, Zarif L. Posaconazole-loaded cyclodextrin nanosponges embedded in Carbopol hydrogel for improved topical delivery. J Drug Deliv Sci Technol. 2025;103:106035. doi: 10.1016/j.jddst.2024.106035

19. Sivadasan D, Ramakrishna K, Mahesh KS, Golla VM, Maheshwari R, Joshi V. Loratadine-loaded nanosponges for enhanced transdermal drug delivery. Asian J Pharm. 2024;18(1):120-131. doi: 10.22377/ajp.v18i1.5289
20. Hani U, Krishna G, Shivakumar HG. Lumiracoxib cyclodextrin nanosponges incorporated in Carbopol-badam gum hydrogel: Development and in vitro evaluation. J Drug Deliv Sci Technol. 2024;94:105507. doi: 10.1016/j.jddst.2024.105507
21. Chopra H, Bibi S, Singh I, Kaur S, Aggarwal G, Alshammari A. Diclofenac diethylamine ethylcellulose nanosponges: Development and characterization for improved topical anti-inflammatory activity. Nanomedicine. 2024;19(4):355-370. doi: 10.2217/nnm-2023-0284
22. Suhail M, Chiu IH, Liu JY, Ullah H, Lin IL, Minhas MU, Tsai MJ, Wu PC. Fabrication and in vitro evaluation of carbopol/polyvinyl alcohol-based pH-sensitive hydrogels for controlled drug delivery. Curr Pharm Des. 2023;29(31):2489-2500. doi: 10.2174/1381612829666231025111343
23. Kane Z, Cheng I, McGarrity O, Chiesa R, Klein N, Cortina-Borja M, Standing JF, Gastine S. Model based estimation of posaconazole tablet and suspension bioavailability in hospitalized children using real-world therapeutic drug monitoring data in patients receiving intravenous and oral dosing. Antimicrob Agents Chemother. 2023;67(7):e00077-23. doi: 10.1128/aac.00077-23
24. Grandhi RS, Perona B. Chiral separation of posaconazole stereoisomers using high-performance liquid chromatography with a cellulose-based column. Biomed Chromatogr. 2025;39(1):e70220. doi: 10.1002/bmc.70220
25. Chen L, Krekels EHJ, Dong Y, Chen L, Maertens JA, Blijlevens NMA, Knibbe CAJ, Brüggemann RJ. Meta-pharmacokinetic analysis of posaconazole following dosing of oral suspension, delayed-release tablet, and intravenous infusion in patients vs. healthy volunteers: Impact of clinical characteristics and race. Int J Antimicrob Agents. 2023;62(6):106995. doi: 10.1016/j.ijantimicag.2023.106995
26. Jansen AME, Snijdelaar K, Keizer RJ, Spriet I, Dreesen E, Brüggemann RJM, Ter Heine R. Personalized antifungal therapy through model-informed precision dosing of posaconazole. Clin Pharmacokinet. 2024;63(5):645-656. doi: 10.1007/s40262-024-01346-7
27. Wiederhold NP. Pharmacokinetics and safety of posaconazole delayed-release tablets for invasive fungal infections. Clin Pharmacol. 2023;15:87-97. doi: 10.2147/CPAA.S420133
28. Cornely OA, Robertson MN, Haider S, Grigg A, Geddes M, Aoun M, Heinz WJ, Raad I, Schanz U, Meyer RG, Hammond SP, Mullane KM, Ostermann H, Ullmann AJ, Zimmerli S, Van Iersel MLPS, Hepler DA, Waskin H, Kartsonis NA, Maertens J. Pharmacokinetics and safety results from the Phase 3 randomized, open-label, study of intravenous posaconazole in patients at risk of invasive fungal disease. J Antimicrob Chemother. 2024;79(1):126-135. doi: 10.1093/jac/dkad263
29. Franco YL, Da Silva L, Charbe N, Kinvig H, Kim S, Cristofoletti R. Population pharmacokinetics and bioavailability of posaconazole: Current insights and future perspectives. Pharm Res. 2023;40(2):405-418. doi: 10.1007/s11095-023-03478-0
30. Jawaharlal S, Subramanian S, Palanivel V, Devarajan G, Veerasamy V. Cyclodextrin-based nanosponges as promising carriers for active pharmaceutical ingredient. J Biochem Mol Toxicol. 2024;38(1):e23597. doi: 10.1002/jbt.23597
31. Kumar A, Sharma V, Singh B, Dhiman V. Development of cyclodextrin nanosponges using melt method for enhanced drug delivery. Drug Deliv Transl Res. 2024;14(3):678-690. doi: 10.1007/s13346-023-01428-2
32. Mohite P, Munde S, Pawar A, Singh S. Unleashing the potential of cyclodextrin-based nanosponges in management of colon cancer: A review. Nanofabrication. 2024;9:1823. doi: 10.37819/nanofab.9.1823
33. Kasparaviciene G, Maslii Y, Herbina N, Kazlauskiene D, Marksa M, Bernatoniene J. Development and evaluation of two-phase gel formulations for enhanced delivery of active ingredients: Sodium diclofenac and camphor. Pharmaceutics. 2024;16(3):366. doi: 10.3390/pharmaceutics16030366
34. Pyrak B, Rogacka-Pyrak K, Gubica T, Szeleszczuk Ł. Exploring cyclodextrin-based nanosponges as drug delivery systems: Understanding the physicochemical factors influencing drug loading

and release kinetics. Int J Mol Sci. 2024;25(6):3527. doi: 10.3390/ijms25063527

35. Omar SM, Ibrahim F, Ismail A. Formulation and evaluation of cyclodextrin-based nanosponges of griseofulvin as pediatric oral liquid dosage form for enhancing bioavailability and masking bitter taste. Saudi Pharm J. 2023;31(5):765-778. doi: 10.1016/j.jsps.2023.03.012
36. Krabicová I, Appleton SL, Tannous M, Hoti G, Caldera F, Rubin Pedrazzo A, Cecone C, Cavalli R, Trotta F. History of cyclodextrin nanosponges. Polymers. 2023;15(5):1122. doi: 10.3390/polym15051122
37. Singh S, Sharma K, Sharma H. Cyclodextrin nanosponges: A revolutionary drug delivery strategy. Pharm Nanotechnol. 2024;12(4):300-313. doi: 10.2174/0122117385273293230927081513
38. Zheng T, Liu C, Wang Y, Zhou R, Wu D, Tan J, Zhu K. Efficacy and safety of topical clobetasol propionate in comparison with alternative treatments in oral lichen planus: an updated systematic review and meta-analysis. Front Med. 2024;11:1391754. doi: 10.3389/fmed.2024.1391754
39. Nair AB, Kumar S, Dalal P, Nagpal C, Dalal S, Rao R, Sreeharsha N, Jacob S. Novel dermal delivery cargos of clobetasol propionate: An update. Pharmaceutics. 2024;16(2):383. doi: 10.3390/pharmaceutics16020383
40. Suhail M, Badshah SF, Chiu IH, Ullah A, Khan A, Ullah H, Al-Sowayan NS, Tsai MJ, Wu PC. A novel approach of polyvinyl alcohol/acrylic acid based hydrogels for controlled delivery of diclofenac sodium. Curr Pharm Des. 2023;29(40):3239-3250. doi: 10.2174/1381612829666231025095713
41. Alhasso B, Ghori MU, Rout SP, Conway BR. Development of a nanoemulgel for the topical application of mupirocin. Pharmaceutics. 2023;15(10):2387. doi: 10.3390/pharmaceutics15102387
42. Kasparaviciene G, Maslii Y, Herbina N, Kazlauskiene D, Marksa M, Bernatoniene J. Development and evaluation of two-phase gel formulations for enhanced delivery of active ingredients: Sodium diclofenac and camphor. Pharmaceutics. 2024;16(3):366. doi: 10.3390/pharmaceutics16030366
43. Li J, Han J, Xiao Y, Guo R, Liu X, Zhang H, Bi Y, Xu X. Fabrication and characterization of novel food-grade bigels based on interfacial and bulk stabilization. Foods. 2023;12(13):2546. doi: 10.3390/foods12132546
44. Suhail M, Chiu IH, Liu JY, Ullah H, Lin IL, Minhas MU, Tsai MJ, Wu PC. Fabrication and in vitro evaluation of carbopol/polyvinyl alcohol-based pH-sensitive hydrogels for controlled drug delivery. Curr Pharm Des. 2023;29(31):2489-2500. doi: 10.2174/1381612829666231025111343
45. Kyser AJ, Mahmoud MY, Herold SE, Lewis WG, Lewis AL, Steinbach-Rankins JM, Frieboes HB. Hydrogel formulations for enhanced mucoadhesive drug delivery. Int J Pharm. 2023;641:123054. doi: 10.1016/j.ijpharm.2023.123054
46. Rotaru-Zăvăleanu AD, Dinescu VC, Aldea M, Gresita A. Hydrogel-based therapies for ischemic and hemorrhagic stroke: A comprehensive review. Gels. 2024;10(7):476. doi: 10.3390/gels10070476
47. Alhasso B, Ghori MU, Rout SP, Conway BR. Development of a nanoemulgel for the topical application of mupirocin. Pharmaceutics. 2023;15(10):2387. doi: 10.3390/pharmaceutics15102387
48. Datta D, Bandi SP, Venuganti VVK. Ionic liquid-mediated transdermal delivery of organogel containing cyclosporine A for the effective treatment of psoriasis. ACS Omega. 2024;9(40):41565-41582. doi: 10.1021/acsomega.4c05346
49. Garshasbi HR, Soleymani S, Naghib SM, Mozafari MR. Multi-stimuli-responsive hydrogels for therapeutic systems: An overview on emerging materials, devices, and drugs. Curr Pharm Des. 2024;30(26):2027-2046. doi: 10.2174/0113816128304924240527113111
50. Sah A, Aggarwal G, Jain GK, Zaidi SMA, Naseef PP, Kuruniyan MS, Zakir F. Novel approaches in hydrogel-based antifungal drug delivery systems. Gels. 2023;9(10):794. doi: 10.3390/gels9100794